OFFICE OF NAVAL RESEARCH

Contract: N00014-85-K-0222

Work Unit: 4327-555

Scientific Officer: Dr. Richard S. Miller

Technical Report No. 20

PLA ⌣ YIELDING OF PARTIALLY-CRYSTALLINE POLYMERS

by

A. N. Gent and S. Madan

Institute of Polymer Science
The University of Akron
Akron, Ohio 44325

May, 1989

SECURITY CLASSIFICATION OF THIS PAGE (When Data Entered)

REPORT DOCUMENTATION PAGE		READ INSTRUCTIONS BEFORE COMPLETING FORM
1. REPORT NUMBER Technical Report No. 20	2. GOVT ACCESSION NO.	3. RECIPIENT'S CATALOG NUMBER
4. TITLE (and Subtitle) Plastic Yielding of Partially Crystalline Polymers		5. TYPE OF REPORT & PERIOD COVERED Technical Report 6. PERFORMING ORG. REPORT NUMBER
7. AUTHOR(s) A.N. Gent and S. Madan		8. CONTRACT OR GRANT NUMBER(s) N00014-85-K-0222
9. PERFORMING ORGANIZATION NAME AND ADDRESS Institute of Polymer Science The University of Akron Akron, Ohio 44325		10. PROGRAM ELEMENT, PROJECT, TASK AREA & WORK UNIT NUMBERS 4327-555
11. CONTROLLING OFFICE NAME AND ADDRESS Office of Naval Research Power Program Arlington, VA 22217-5000		12. REPORT DATE May 1989 13. NUMBER OF PAGES 36
14. MONITORING AGENCY NAME & ADDRESS(if different from Controlling Office)		15. SECURITY CLASS. (of this report) Unclassified 15a. DECLASSIFICATION/DOWNGRADING SCHEDULE

16. DISTRIBUTION STATEMENT (of this Report)

According to attached distribution list.
Approved for public release; distribution unrestricted.

17. DISTRIBUTION STATEMENT (of the abstract entered in Block 20, if different from Report)

18. SUPPLEMENTARY NOTES

Submitted for publication in: J. Polymer Sci.: Part B: Polymer Physics

19. KEY WORDS (Continue on reverse side if necessary and identify by block number)

Crystalline, Deformation, Drawing, Plastic, Polymers, Strain, Tension, Yielding

20. ABSTRACT (Continue on reverse side if necessary and identify by block number)

Measurements are described of characteristic stress-strain properties in tension for several representative partially-crystalline polymers, prepared by cooling from the melt. Striking differences were found in the natural draw ratio, ranging from 2X to 11X. They are interpreted in terms of a simple

DD FORM 1 JAN 73 1473 EDITION OF 1 NOV 65 IS OBSOLETE
S/N 0102-LF-014-6601

SECURITY CLASSIFICATION OF THIS PAGE (When Data Entered)

molecular model of the yielding process in which polymer chains, folded to different degrees in the crystallites, are pulled taut. Values of yield and draw stress were found to be of the same order as the free energy U_m of melting, suggesting that yielding and drawing take place by stress-induced disruption of crystallites, analogous to melting. The mechanical work of drawing was similar to, but generally larger than, that required for melting, ranging from U_m to about $4U_m$. The difference is attributed to strain energy of drawn material and possible recrystallization during drawing.

1. Introduction

Although much is known about the microstructure of semi-crystalline polymers, there is surprisingly little published work dealing with their physical properties in a quantitative way. As pointed out previously (1), they show remarkable differences in ductility. High-density polyethylene has a natural draw ratio of about 10X whereas trans-polyisoprene has a natural draw ratio of only about 3X. Other examples are given below. These differences do not seem to be due solely to differences in crystallinity. Indeed, the more crystalline materials appear to have generally higher natural draw ratios, contrary to expectation. It has been suggested, instead, that the extensibility of crystalline polymers is related to the degree of molecular chain folding within the crystallites; highly-folded chains being capable, at least in principle, of large extensions (1,2).

A second important property of crystalline plastics is their yield stress, i.e., the maximum stress that they can withstand before the onset of general plastic deformation. Again, although different polymers show markedly different yield stresses, there does not appear to be a generally-accepted connection between the microstructure and resistance to yielding. Some comparative measurements of yield and draw stresses have therefore been made for a number of common semi-crystalline plastics, over a broad temperature range. They are reported here, and compared with predictions of a simple theoretical model, in which drawing is attributed to stress-induced "melting". The principal factors affecting the yield and draw stresses are thus

the degree of crystallinity and the free energy of melting.

A similar hypothesis was put forward by Duska and Harrison (3,4). They focussed attention on the maximum elastic strain energy that the material can support before yielding, and implied that it is correlated with the heat of fusion, but they did not propose a quantitative relationship between the two parameters. Popli and Mandelkern (5) also summarized evidence in favor of stress-induced melting, at least in part, as a mechanism of plastic yielding in polyethylene, but again did not propose a quantitative relationship.

Hartman, Lee and Cole suggested a strain energy criterion for yielding in semi-crystalline polymers, principally to account for the temperature dependence (6). However, their treatment does not deal with the mechanism of deformation considered here, by disrupting crystallites.

Glassy polymers also yield, in a superficially similar way, but on a smaller scale, confined to narrow shear bands or to microscopic crazes, and at considerably higher stresses. A broadly-similar hypothesis to that put forward here for plastic yielding and drawing in crystalline polymers was proposed previously to account for the phenomenon of crazing (7). A stress-induced transition from the glassy state to a rubbery or liquid state was shown to account for several aspects of crazing; notably, the relation between strength and molecular weight (8), and "environmental stress cracking", i.e. the tendency of certain fluids that are rather poor solvents for the polymer to lower the stress level at which crazes appear (7). We now examine the hypothesis of a stress-induced phase

transition, i.e., melting, as the mechanism of ductile deformation of semi-crystalline polymers above their glass transition temperatures.

2. Experimental details

Several semi-crystalline polymers were employed in this study : high and low density polyethylene (HDPE and LDPE), polypropylene (PP), polycaprolactone (PCL), polybutene-1 (PB), trans-polyisoprene (TPI), lightly-crosslinked trans-polychloroprene (TPC), and polytetrafluoroethylene (PTFE). Details of the materials are given in the Appendix.

In each case the polymer was molded as a sheet, about 0.8 mm thick, in a hot press at a temperature above the melting temperature for a period of about one hour. The molded sheet was then cooled rapidly to room temperature, about 20°C.

Dog-bone-shaped samples, having a parallel-sided central portion about 20 mm long and 2 mm wide, were cut from the molded sheets. They were stretched at various rates in a tensile test machine, at temperatures between -40°C and 160°C . A schematic relation between tensile force and displacement of the ends of the sample is shown in Figure 1 ,with sketches of the sample at different stages of deformation.

Several physical properties were determined from the experimentally-determined stress-strain relations: the yield stress σ_y at which the tensile force passed through a maximum, the draw stress σ_d , sometimes appreciably lower than the yield stress, the natural draw ratio λ_d, i.e., the constant extension ratio in the drawn part of

the sample as the neck propagated, transforming undrawn material into the drawn state , and the breaking stress, denoted σ_b. Results obtained at room temperature are given in Table 1. In all cases, stresses refer to the original (unstrained) cross-sectional area of the sample.

Estimates of the degree of crystallinity $\underline{c}$ of each sample were obtained from measurements of the heat of fusion by DSC, using reported values of the heat of fusion $\underline{h}$ of 100 percent crystalline material. They are included in Table 1.

3. Experimental results and discussion

(i) Nature of plastic yielding in crystalline polymers

Although the general pattern of plastic yielding has been described many times, some features do not seem to have been pointed out previously. The characteristic neck first appears at an angle β of about 55° to the direction of tension, rather than at 90°, as shown in Figure 2a. This feature was particularly clear in harder materials such as HDPE, PP, PCL, and TPI. It is in good agreement with the criterion, $\cos 2\beta = -1/3$, given by Bowden (9) for neck formation without change in one dimension, a condition imposed by the rigidity of the still unyielded material on either side of the nascent neck. Then, as the neck propagates, the constraint imposed by neighboring material diminishes and the angle β changes to 90°, Figure 2b.

In TPI, propagation of the neck could be seen to take place intermittently, by periodic movement of a band of material from the undrawn part into the drawn part, forming characteristic striations, Figure 3. This process continued from the initial formation of a neck until drawing was complete. It indicates that the drawing process is not homogeneous but involves discrete portions of material, taken successively to the fully-drawn state.

Similar details of the drawing process were not observable in other polymers, like LDPE, which formed a neck more gradually, and at significantly larger strains (5). Indeed, at low rates of strain, below about $1 \times 10^{-3} s^{-1}$, TPC, PB, and LDPE extended more or less uniformly, without forming a visible neck.

(ii) Physical properties

Striking differences were found in the physical properties of the different polymers, as shown by the results given in Table 1. Values of the natural draw ratio λ_d ranged from 2 to 10. Yield stresses ranged from 7 to 21 MPa at room temperature, and draw stresses varied similarly, lying somewhat below the yield stress.

As the test temperature was varied, the draw ratio was found to remain substantially unchanged but the yield and draw stresses decreased sharply with increasing temperature. Typical relations are shown in Figures 4 and 5. For several materials, the dependence was approximately a linear one, Figure 4, and the yield and draw stresses fell to zero at the melting temperature of the sample, somewhat below the thermodynamic melting temperature, given in Table 1. For PP, HDPE, LDPE and PTFE, the yield and draw stresses followed a non-linear dependence on temperature, as shown in Figure 5, but they still fell to zero at a temperature, obtained by extrapolation, close to the melting temperature. We now turn to the physical interpretation of these results.

(iii) Natural draw ratio, breaking extension, and recovery from the drawn state

Employing the concept put forward previously, that drawing takes place by straightening crystalline and amorphous molecular sequences, the observed values of natural draw ratio λ_d can be interpreted in terms of the number f of times that a molecule passes through the same crystallite (1):

$$1/\lambda_d = (c/f) + (1 - c)^{1/2}/n^{1/2}. \qquad (1)$$

where n denotes the number of equivalent random links between points

f molecular entanglement in the melt, typically between 100 and 500. Values of f were calculated in this way from the measured natural draw ratios. They were approximately 1 for TPI, TPC, and PE, indicating little or no re-entry into the same crystallite, and 2 to 4 for LDPE, PTFE, PP, and PCL, indicating a limited amount of molecular reversal and re-entry. For HDPE the value of f was relatively large, about 11, suggesting that a substantial degree of chain folding occurred in this case. But it is noteworthy that HDPE was quite unusual in this respect, reflecting an unusually high natural draw ratio (10).

After reaching the fully-drawn state, samples could then be extended further, now homogeneously, until the breaking stress and strain were reached. The extension at break was found to be generally about twice as large as the extension attained in drawing. Thus, HDPE, which had a natural draw ratio of about 10X, finally broke at a tensile strain of about 18, and PCL, which drew by a factor of 5X, broke at an extension of about 10.

It is clear that substantial further rearrangement of crystalline and amorphous material can take place after the natural draw ratio has been reached. Previously it was proposed that the natural draw ratio is that deformation at which molecules that happen to traverse a crystallite unfavorably, with their entangled junctions at opposite sides and lying in the direction of the applied tension, become fully stretched (1). Other molecules, more favorably situated, will reach the fully-stretched state later. Thus, extensive molecular rearrangement after the natural draw ratio is reached, permitting further extension of drawn material, is not incompatible

with the principal mechanism of drawing.

Measurements were also made of the retraction of drawn samples on heating. When the tension was released, the immediate recovery was quite small, less than 10 percent of the imposed extension. On warming, the samples began to retract, as shown in Figure 6, and recovery was virtually complete at the melting temperature.

There was one outstanding exception, however. Samples of PCL showed much less recovery, retaining more than one-half of the imposed strain at the melting point. This feature is tentatively attributed to unusually low molecular weight of the PCL sample, only about 40,000 g/mole. Extensive slippage of entangled molecules may well take place in this case during drawing. If this is so, then the inferred value of $\underline{f}$ for PCL, about 3, will be too high because the natural draw ratio has been over-estimated.

(iv) Theoretical interpretation of yield and draw stresses

We consider first the relationship between the draw stress and the thermodynamic work of melting, $\underline{U}_m$, given by (11)

$$U_m = c\ \rho\ h\ (1 - T/T_m), \qquad (2)$$

where c is the fractional degree of crystallinity, ρ is the density, $\underline{h}$ is the heat of fusion of 100 percent crystalline material, T is the test temperature and T_m is the crystal melting temperature. Values of these parameters are given in Table 1 for each polymer.

Experimental values of the draw stress σ_d are plotted in Figure 7 against calculated values of the work of melting U_m. The results are seen to fall into two groups: polymers with low values of natural draw ratio show rather good agreement between draw stress and the work

of melting. Whereas polymers with large natural draw ratios have much lower draw stresses, compared to the work of melting, only about one-fifth as large in the case of HDPE.

Similar conclusions are reached if yield stresses are considered instead of draw stresses. Values of yield stress σ_y are plotted against the thermodynamic work of melting in Figure 8. Again, polymers with low natural draw ratios, between 2 and 3, show satisfactory agreement between yield stress and the work of melting, whereas polymers having high ductility; for example, HDPE; have much lower yield stresses for equivalent values of U_m.

These differences between different polymers can be attributed to different energies of deformation, even for the same yield and draw stress. In the following section the work expended in drawing is compared to the free energy of melting. (A similar comparison is not made for yielding because the yield stress depends significantly upon the rate of stretching, as discussed later.)

Although significant differences are present, as pointed out above, surprisingly good numerical agreement is obtained between observed yield and draw stresses and the computed work of melting for a number of polymers. This empirical observation suggests that the hypothesis of Juska and Harrison is basically correct. However, it is thought that their estimate of the work required to bring about the melting transformation is inappropriate, as discussed below.

(v) Work expended in plastic drawing

When plastic deformation occurs, energy is expended in drawing, given by the product of the draw stress and the extension accompanying drawing,

$$U = \sigma_d(\lambda_d - 1) \quad . \qquad (3)$$

It is proposed here that the criterion for drawing is that this mechanical work is enough to disrupt the crystallites completely, i.e., $\underline{U} = \underline{U}_m$. This criterion differs somewhat from that proposed by Juska and Harrison (3,4), who employed the strain energy stored in the material at the onset of yielding as a measure of the work of melting.

Now, because several polymers have values of $\underline{\lambda}_d$ of the order of 2 to 3, the corresponding work of drawing will lie between $\underline{\sigma}_d$ and $2\underline{\sigma}_d$, Equation 3. Thus, the degree of agreement found between the draw stress itself and the work of melting for these polymers is not so surprising. On the other hand, for PP, LDPE, and HDPE, with values of $\underline{\lambda}_d$ ranging between 4.5 and 10, the work of drawing $\underline{U}$ becomes a larger multiple of the draw stress and hence the draw stress itself will be a smaller fraction of the thermodynamic work of melting $\underline{U}_m$, as is observed (Figures 7 and 8).

Approximate values of the effective draw strain $\underline{e}_d^*$ can be deduced by comparing measured draw stresses with those predicted by Equations 2 and 3. They are listed in Table 2 and compared with the actual draw strains for each polymer. As can be seen, although the two values are of the same order, the effective draw strain and thus the work required to melt the polymer is generally lower than the work actually expended in drawing. In other words, the amount of mechanical work expended in drawing is similar to, but generally larger than that needed to melt crystalline material, by a factor between 1X and 4X.

Two possible reasons for this discrepancy can be put forward. Work of elastic deformation accompanying drawing has not been taken into account, although it is clearly present when drawn material is heated to the melting point and retracts to the unstrained state. And it is possible, at least for materials well below the melting point, that they recrystallize during drawing, before reaching the fully-drawn state. In this case, work of melting must be provided more than once during drawing. Unfortunately, neither of these effects are easily quantified. Either of them would cause the work of drawing to exceed the value calculated from Equations 2 and 3.

(vi) Effect of rate of deformation on yielding

It is helpful, again, to consider the polymers studied here in two groups. The first, those polymers having values of natural draw ratio between 2 and 3 showed very little dependence of the yield stress and draw stress on rate of deformation, Figures 9 and 10. Indeed, it should be noted that yield stresses and draw stresses were quite similar for these polymers.

The second group of polymers, having large values of natural draw ratio, showed a steady increase in yield stress with rate of deformation, Figure 9. At first sight, this dependence is inconsistent with the thermodynamic concept of stress-induced melting, taking place, in principle, at equilibrium. However, the work of deformation $\underline{U}$ employed here is obtained from drawing, and comparison is made of draw stress and draw ratio with theoretical predictions, rather than yield stress. And the draw stress was found to be less sensitive to rate of deformation, Figure 10. It is therefore

thought that a pronounced dependence of yield stress on rate of deformation does not vitiate the proposed mechanism of drawing by a stress-induced phase transition. But, clearly, further study is required of differences between yield stress σ_y and draw stress σ_d. They are particularly different for polymers with high natural draw ratios, stretched at high rates.

(vii) Polytetrafluoroethylene, PTFE

Yield and draw stresses for PTFE were remarkably low in comparison with estimated values of the work of melting, Figures 7 and 8. These results cannot be attributed to an excesively high degree of ductility for PTFE. On the contrary, the natural draw ratio was relatively low, about 3.3. Instead, it must be hypothesised either that the mechanism of yielding is distinctly different for PTFE, or, as seems more likely, that the effective melting temperature at which the structure flows under stress is much below the reported melting temperature. Intermediate melting transitions have been reported for PTFE (12,13).

4. Conclusions

The following conclusions are obtained:

Several polymers, with low values of natural draw ratio, show good agreement between measured yield or draw stresses and those calculated from the work of melting. This empirical observation is regarded as good evidence for the basic Juska and Harrison hypothesis, that yielding is associated with stress-induced melting.

It is proposed that the work of drawing is primarily expended in meeting the thermodynamic requirements of melting. In accordance with this concept, the product $\underline{\sigma}_d\underline{e}_d$ of the measured draw stress and natural draw strain is found to be of the same order as the free energy of melting. Numerical values range from 1X to 4X of the theoretical amount of work required to melt the material. Possible reasons for the discrepancy are that additional energy is expended in elastic deformation, and that recrystallization occurs during drawing.

Attention is focussed on draw stress and work of drawing, rather than yield stress and work of yielding. For polymers with low natural draw ratios, between 2 and 3, the distinction is unimportant because the yield stress and draw stress are quite similar. For polymers with higher natural draw ratios, notably low- and high-density polyethylenes, the yield stress is considerably higher than the draw stress, and more so at higher rates of deformation. Indeed, the dependence of the yield stress upon rate of straining, and upon time under load (14), suggests that it is not amenable to direct thermodynamic interpretation.

Acknowledgements

This work was supported by research grants from the Office of Naval Research (Contract No. N00014-85-K-0222) and Lord Corporation. The authors are also indebted to Dr. W. Sung for helpful discussions on the thermodynamics of melting.

References

1. A. N. Gent and J. Jeong, Polym. Eng. Sci. 26, 285-289 (1986).
2. W. O. Statton, J. Appl. Phys. 38, 4149-4151 (1967).
3. T. Juska and I. R. Harrison, Polym. Eng. Reviews 2, 13-28 (1982).
4. T. Juska and I. R. Harrison, Polym. Eng. Sci. 22, 766-776 (1982).
5. R. Popli and L. Mandelkern, J. Polym. Sci.: Part B: Polym. Phys. 25, 441-483 (1987).
6. B. Hartmann, G. F. Lee and R. F. Cole, Jr., Polym. Eng. Sci. 26, 554-559 (1986).
7. A. N. Gent, J. Mater. Sci. 5, 925-932 (1970).
8. A. N. Gent and A. G. Thomas, J. Polym. Sci., Part A-2 10, 571-573 (1972).
9. P. B. Bowden, Chap. 5 in "The Physics of Glassy Polymers," ed. by R. N. Haward, John Wiley & Sons, N.Y., 1973, p. 311.
10. G. Meinel and A. Peterlin, Europ. Polym. J. 7, 657-670 (1971).
11. L. Mandelkern, "Crystallization of Polymers," McGraw-Hill, New York, 1964, p. 40.
12. H. W. Starkweather, J. Polym. Sci. Polym. Phys. Ed. 17, 73-79 (1979).
13. S. K. Lau, H. Suzuki and B. Wunderlich, J. Polym. Sci. Polym. Phys. Ed. 22, 379-405 (1984).
14. J. M. Crissman and L. J. Zapas, Polym. Eng. Sci. 19, 99-103 (1979).

Appendix

The following materials were used in the experiments.

High-density polyethylene (HDPE): Microsuntec R340P, from Asahi-Kasei Ind., Japan. Density, 0.955 g/ml; melt index, 7 g/10 min.

Low-density polyethylene (LDPE): Flothene G801, from Asahi-Kasei Ind., Japan. Density, 0.920 g/ml; melt index, 20 g/10 min.

Polypropylene (PP): PP 4092, from Exxon Chemical Company. Density, 0.90 g/ml.

Polycaprolactone (PCL): PCL-700, from Union Carbide Corp. Density, 1.149 g/ml at 20°C; wt. av. mol. wt., 4×10^4 g/mole.

Polybutene-1 (PB): PB 8240, from Shell Chemicals.

Polytetrafluoroethylene (PTFE): Hoerst TFM 1600, from Pfaudler-Edlon Products. Density, 2.17 g/ml.

Trans-polyisoprene (TPI): Trans-PIP 301, from Polysar Limited, Canada.

Trans-polychloroprene (TPC): Neoprene HC, from E. I. duPont de Nemours and Co. This material was lightly crosslinked, using the following mix formulation, by heating for 1 h at 150°C. Neoprene HC, 100; extra light calcined magnesia, 4; zinc oxide, 5; Permalux (accelerator), 0.5; Antioxidant 2246, 1.

Table 1: Thermodynamic parameters and tensile properties at 25°C for eight semi-crystalline polymers.

Polymer	Heat of fusion h(kJ/kg)	Melting temperature T_m (°C)	Density ρ(g/ml)	Crystallinity C (%)	Draw ratio λ_d	Yield stress σ_y(MPa)	Draw stress σ_d(Mpa)	Stress at break σ_b(MPa)
HDPE	290	130	0.95	60	10.2	21	13	21
LDPE	290	120	0.917	31	4.5	9	9	10.5
PP	210	180	0.90	48	6.0	15[a]	11.5[a]	39[a]
PCL	136	70	1.15	59	5.3	18	13	38
PB	120	120	0.91	48	2.0	14	14	36
TPI	186	70	0.95	28	2.3	9	8	40
TPC	95	75	1.29	30	2.7	7	7	30.5
PTFE	63	335	2.17	67	3.3	13	12	37.5

[a]measured at 60°C.

Table 2: Comparison of measured draw strain $e_d (= \lambda_d - 1)$ with effective value e_d^*, calculated from draw stress and work of melting, Equations 2 and 3.

Polymer	e_d	e_d^*
PB	1.0	1.0
TPI	1.3	0.9
TPC	1.7	0.9
PTFE	2.3	4.5
LDPE	3.5	2.5
PCL	4.3[a]	1.0
PP	5.0	3.0
HDPE	9.2	3.0

[a]draw strain not fully recoverable, see text.

Figure Legends

Figure 1: Relation between tensile stress and mean elongation ratio, given by the overall length of the sample relative to its initial length.

Figure 2: Formation and propagation of a neck in trans-polyisoprene (TPI).

Figure 3: Striations in drawn trans-polyisoprene (TPI).

Figure 4: Yield stress σ_y (open points) and draw stress σ_d (filled-in points) for PCL (O,●) and TPC (□,■), plotted against test temperature T. Rate of extension: $\dot{e} = 0.015\ s^{-1}$

Figure 5: Yield stress σ_y (open points) and draw stress σ_d (filled-in points) for HDPE (△,▲) and LDPE (▽,▼), plotted against test temperature T. Rate of extension: $\dot{e} = 0.015\ s^{-1}$

Figure 6: Residual strain e vs temperature for several polymers, drawn at 20°C to strains exceeding their natural draw strain and then released and heated.

Figure 7: Draw stress σ_d vs free energy U_m of melting. ⬢, TPI; ●, PCL; ◆, PB; ■, TPC; X, PP; ▼, LDPE; ▲, HDPE; ▶, PTFE. The broken line represents $\sigma_d = U_m$.

Figure 8: Yield stress σ_y vs free energy U_m of melting. ⬡, TPI; O, PCL; ◇, PB; □, TPC; +, PP; ▽, LDPE, △, HDPE. The broken line represents $\sigma_y = U_m$.

Figure 9: Yield stress σ_y at 25°C vs rate of extension $\dot{e}$.

+, PP; △, HDPE; O, PCL; ◇, PB; ▷, PTFE; ⬡, TPI; □, TPC.

Figure 10. Draw stress σ_d at 25°C vs rate of extension $\dot{e}$.

X, PP; ▲, HDPE; ●, PCL; ◆, PB; ▶, PTFE; ⬢, TPI; ■, TPC.

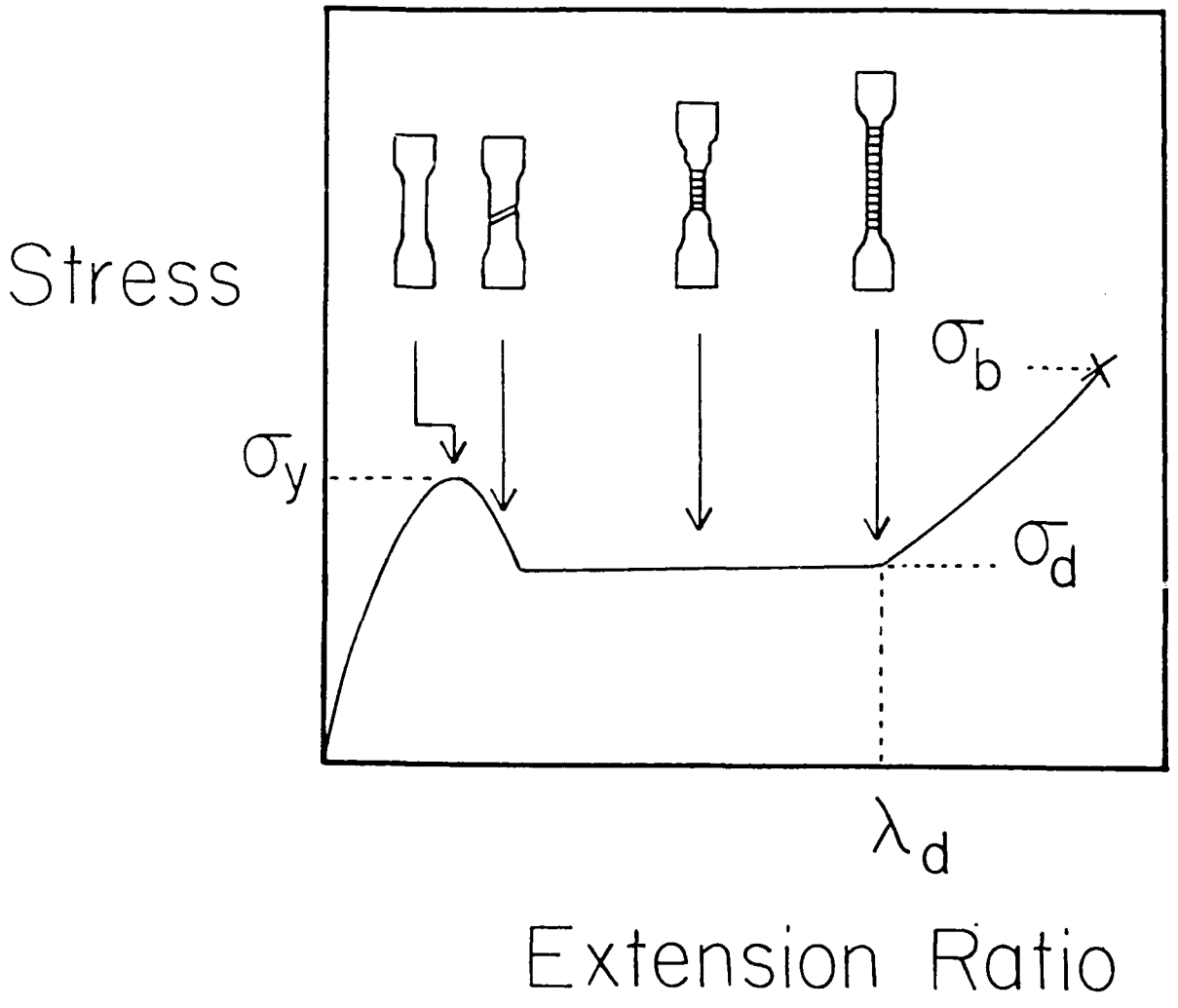

Figure 1

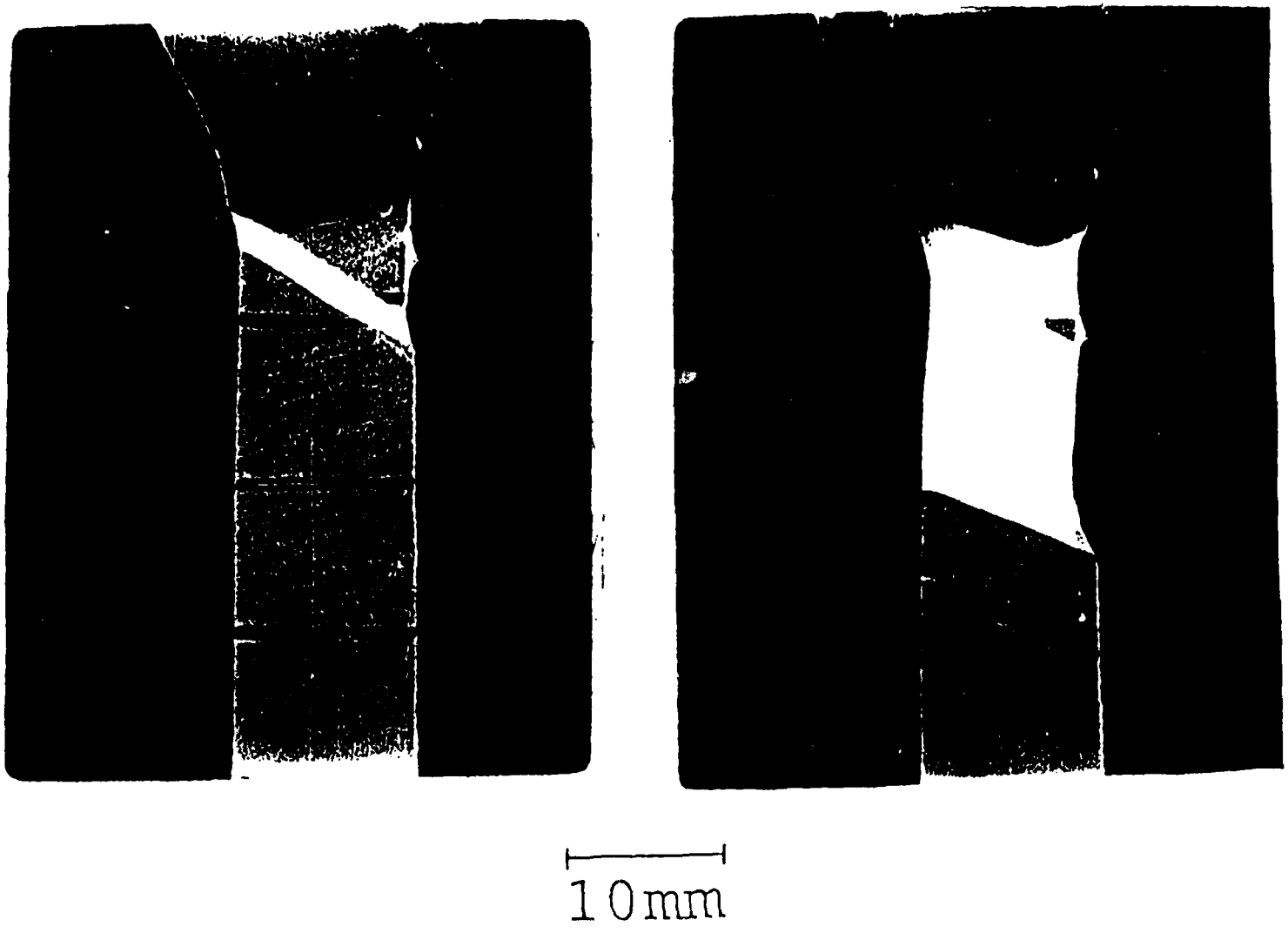

Figure 2

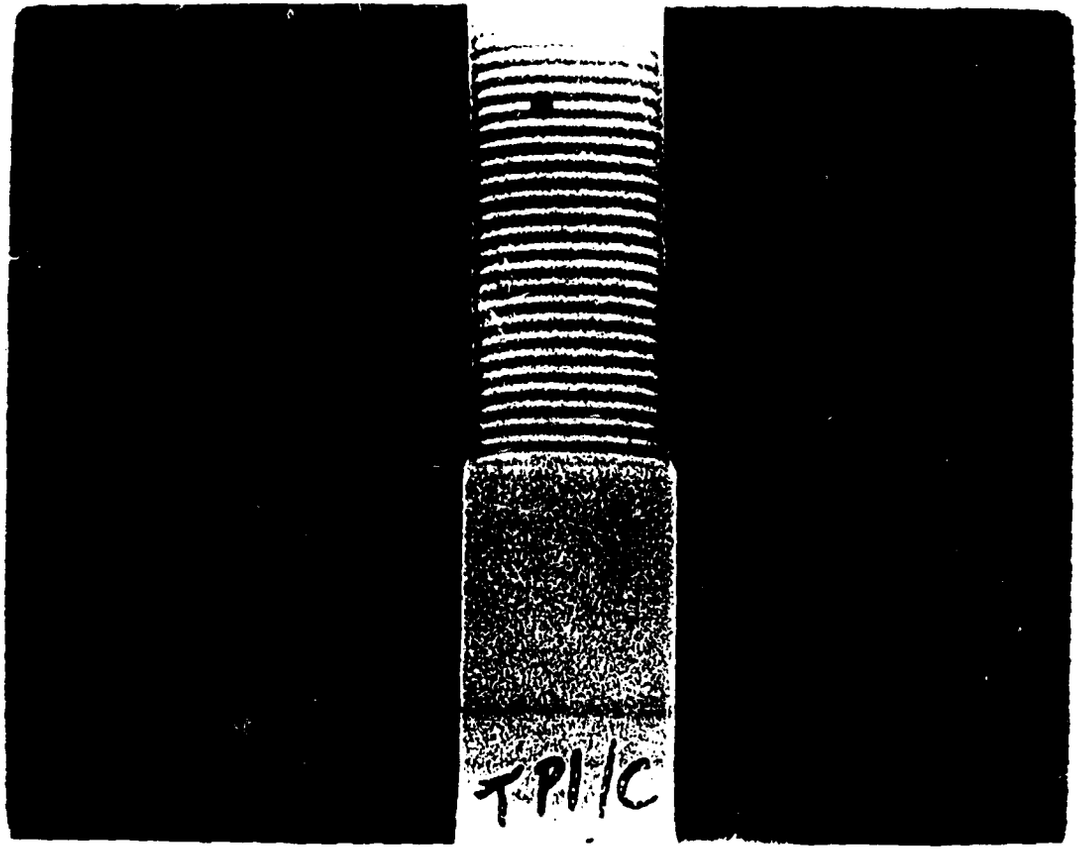

Figure 3

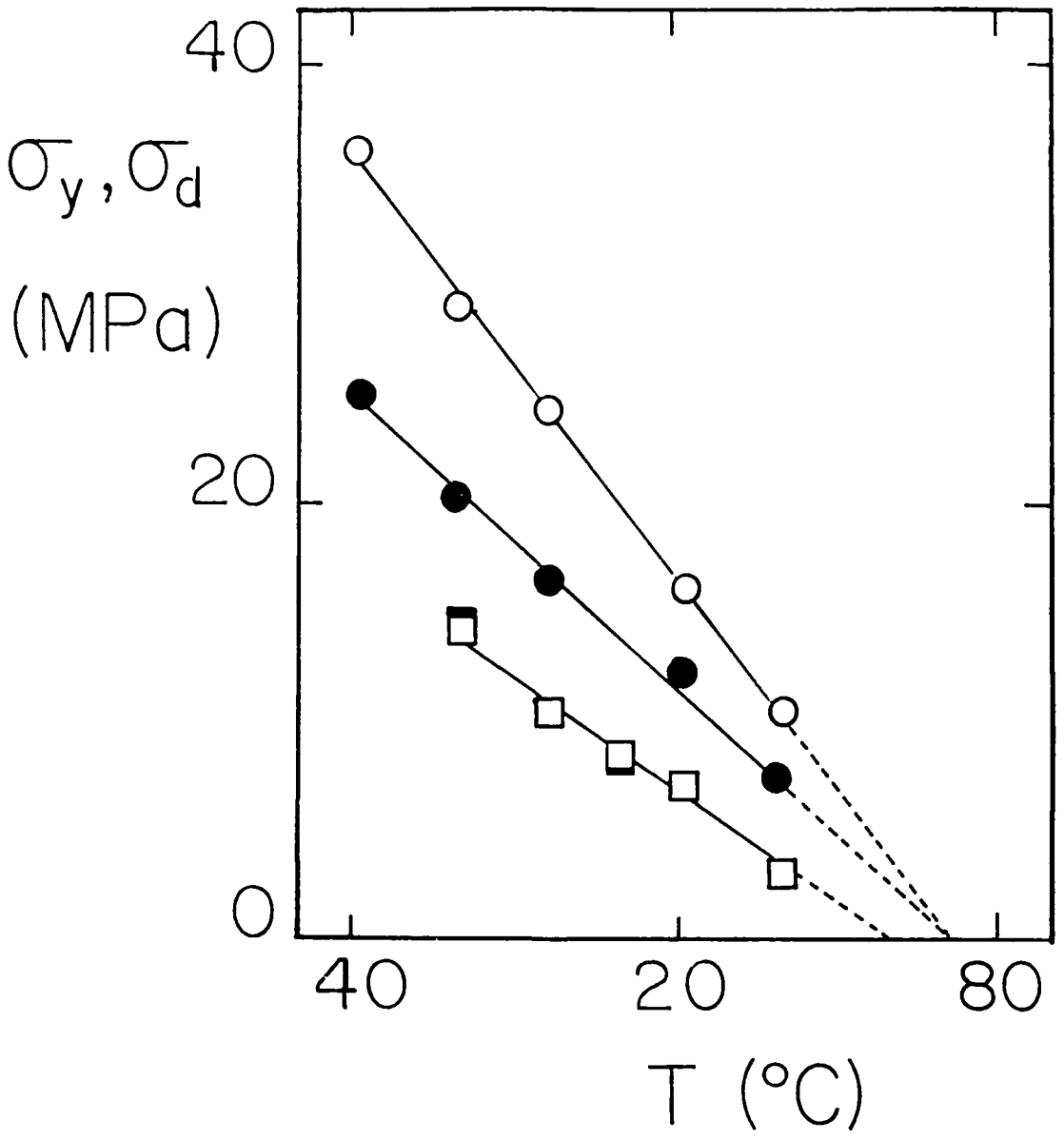

Figure 4

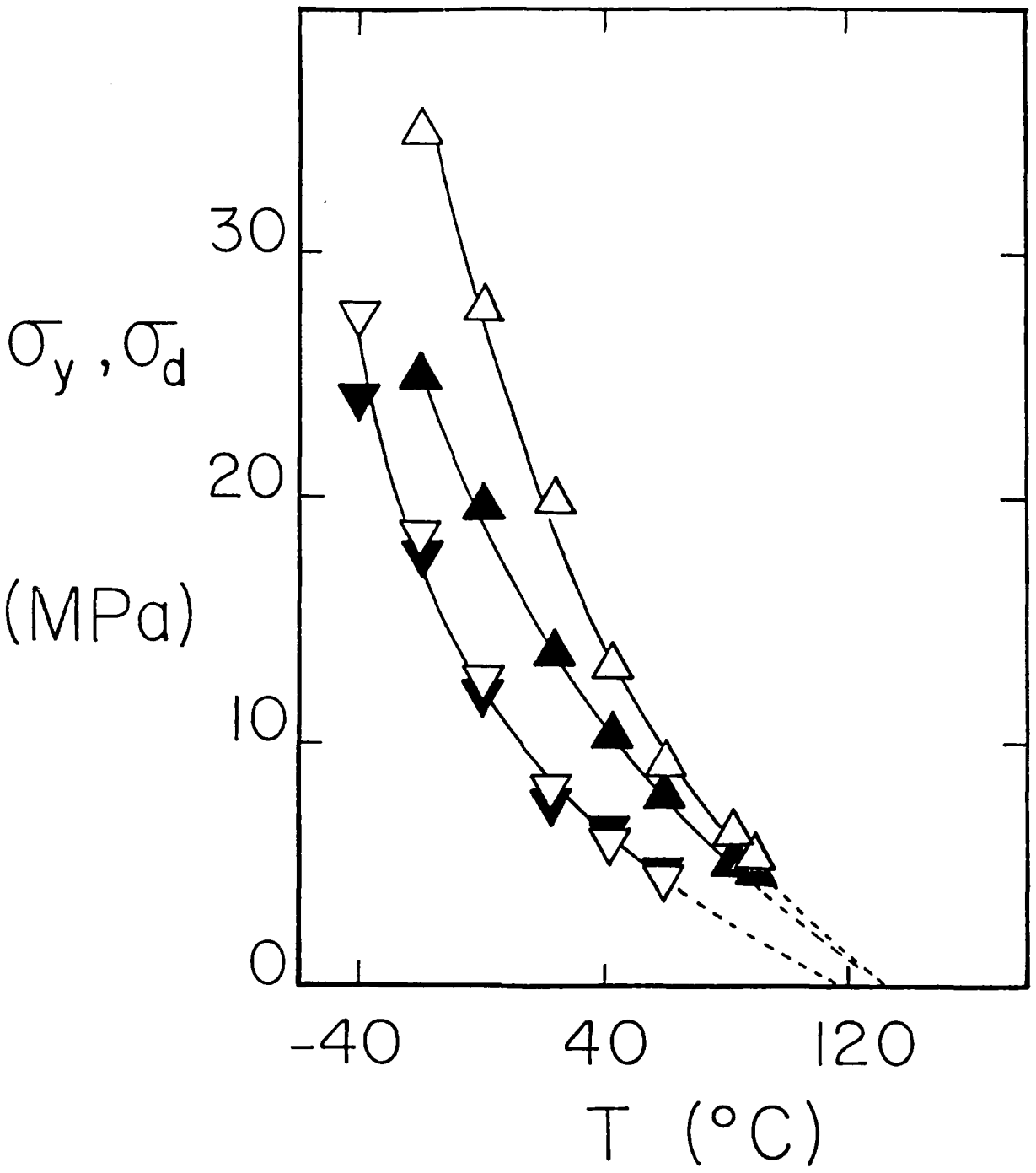

Figure 5

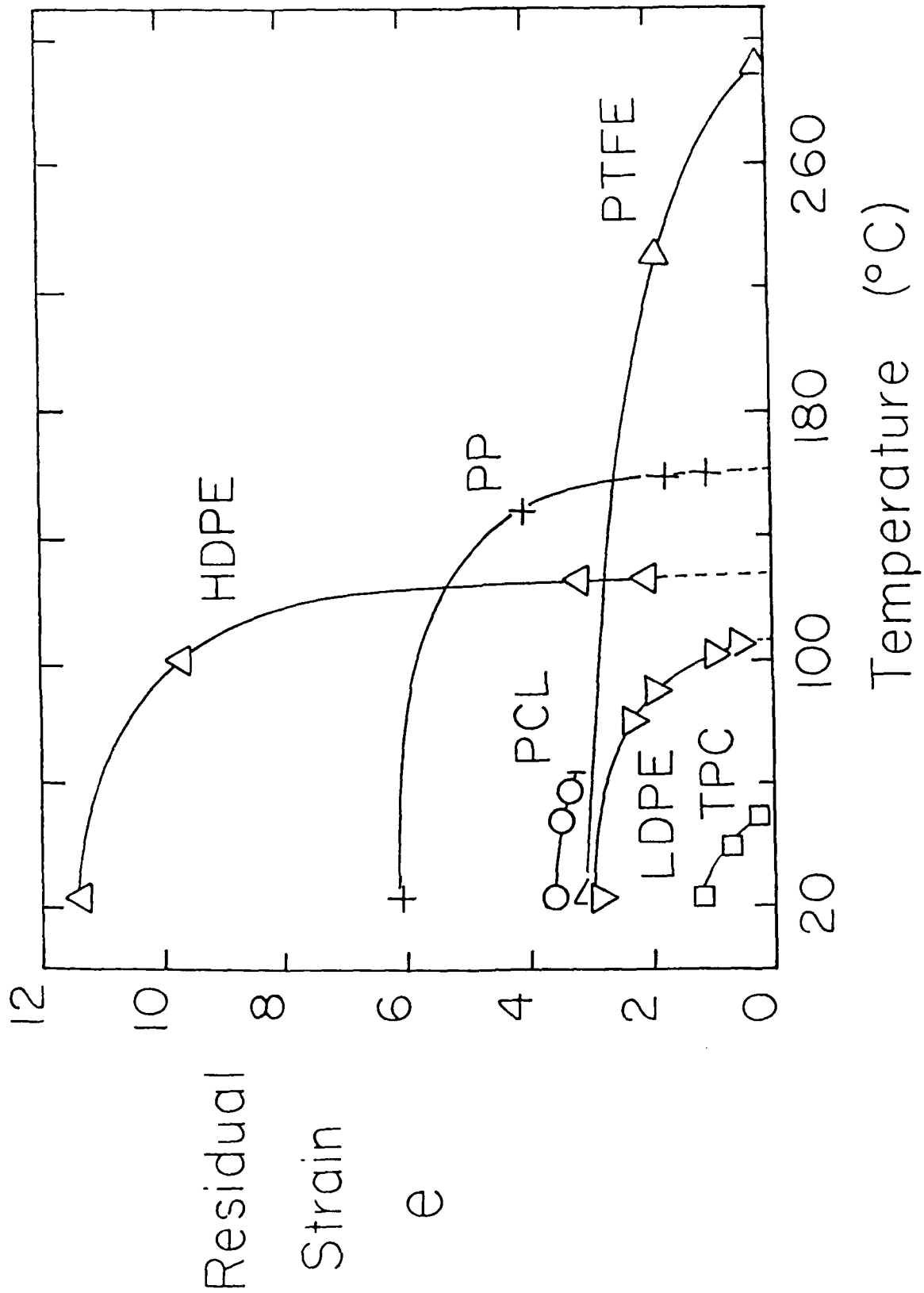
Residual Strain e
0
2
4
6
8
10
12
20
100
180
260
Temperature (°C)
HDPE
PP
PTFE
PCL
LDPE
TPC

Figure 6

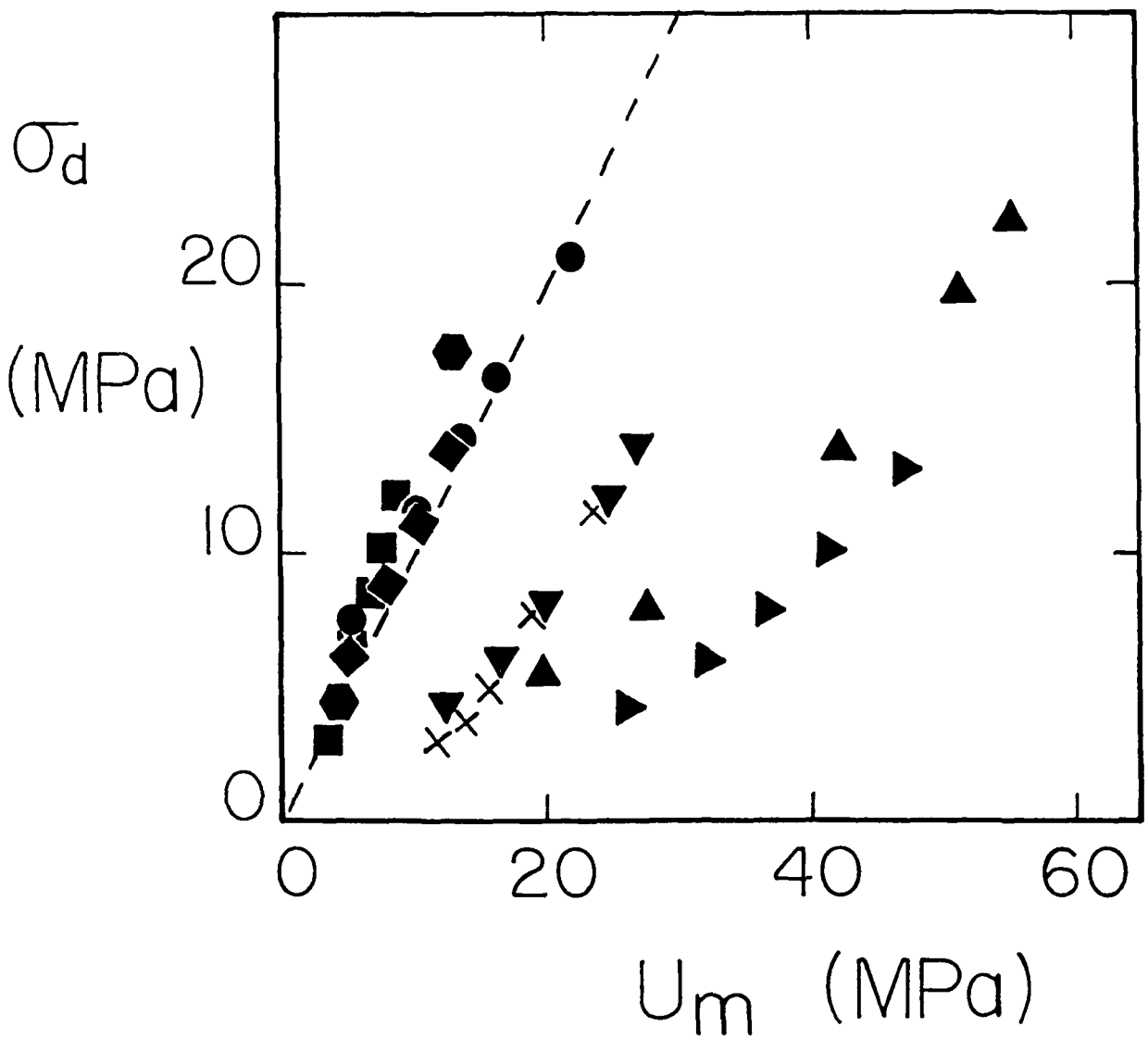

Figure 7

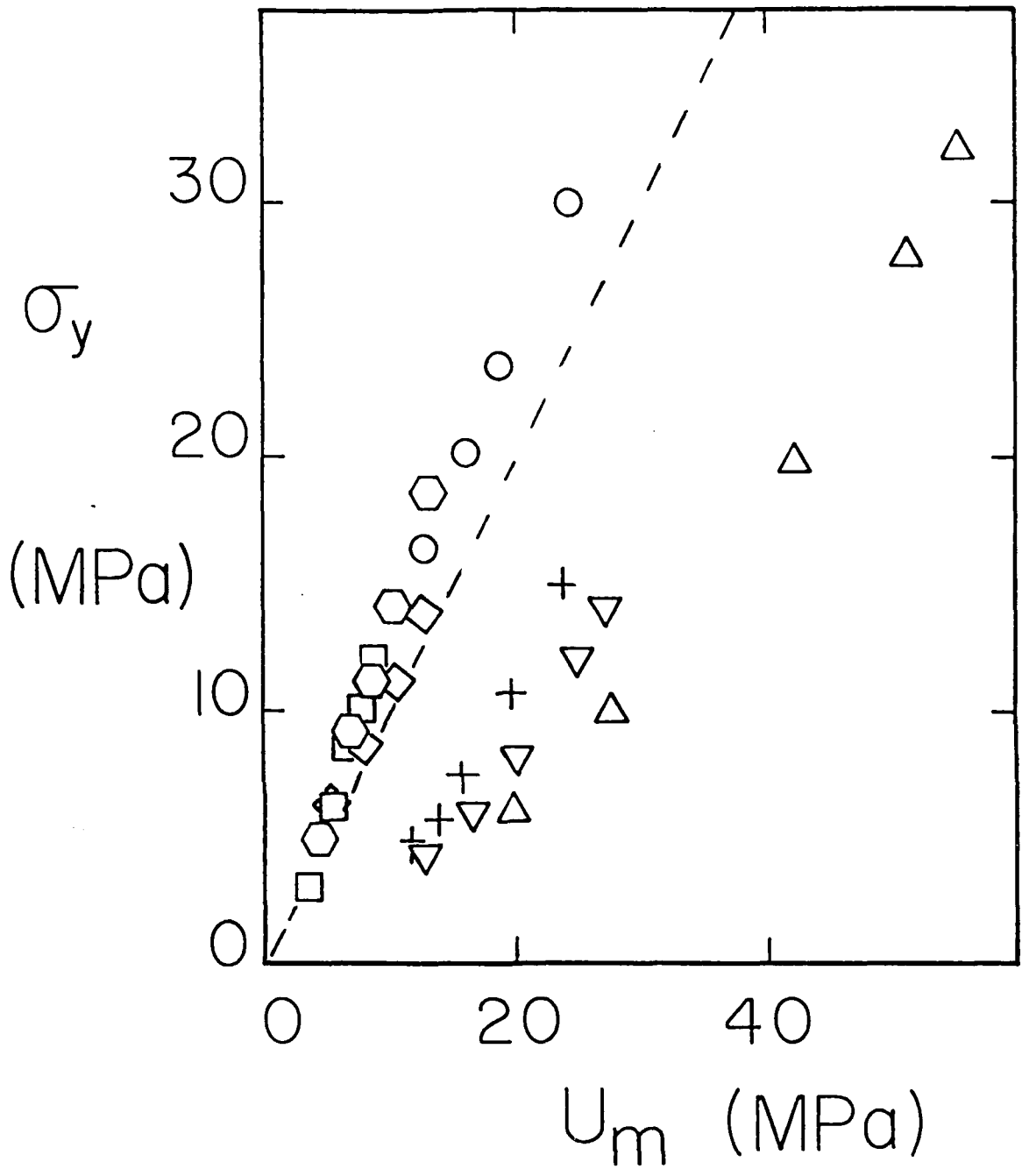

Figure 8

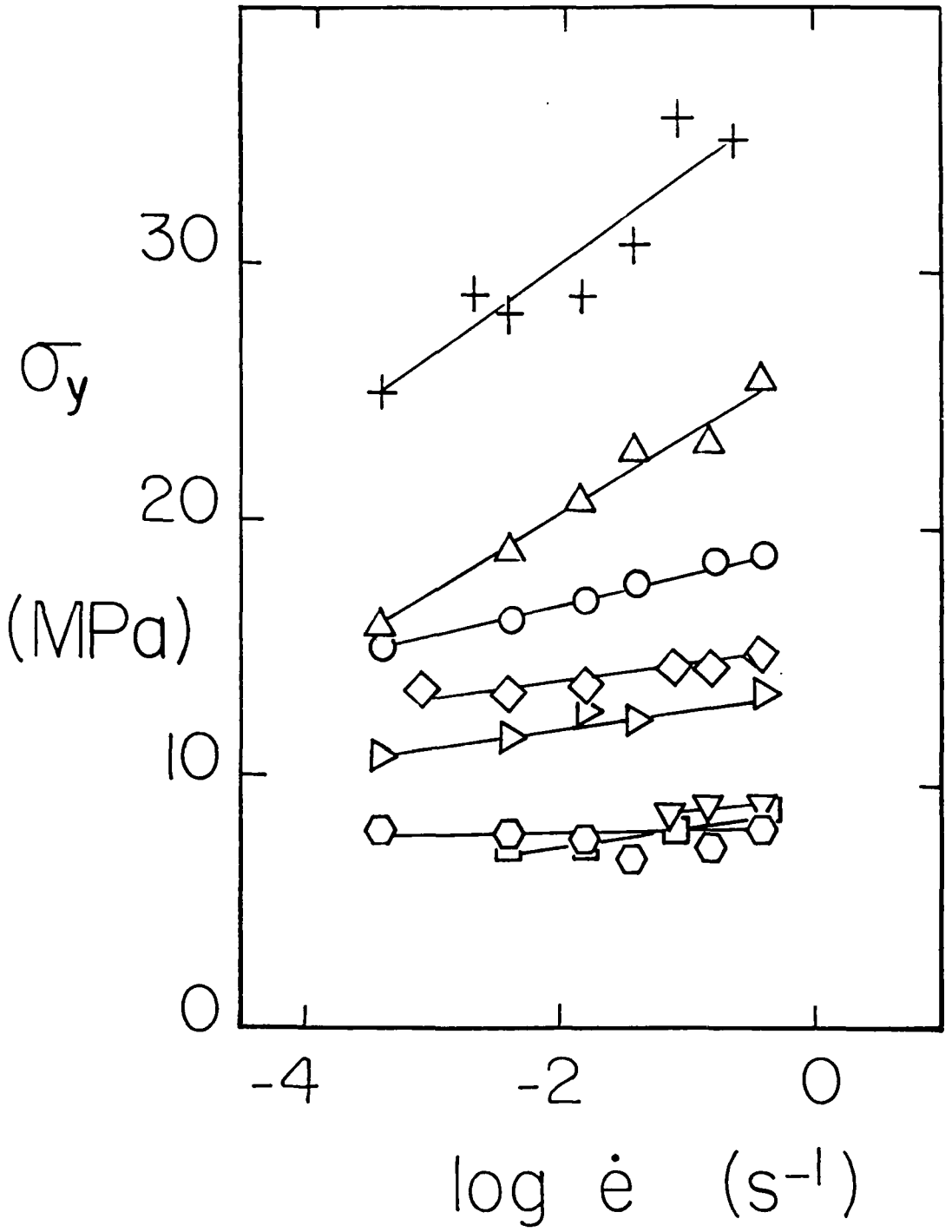

Figure 9

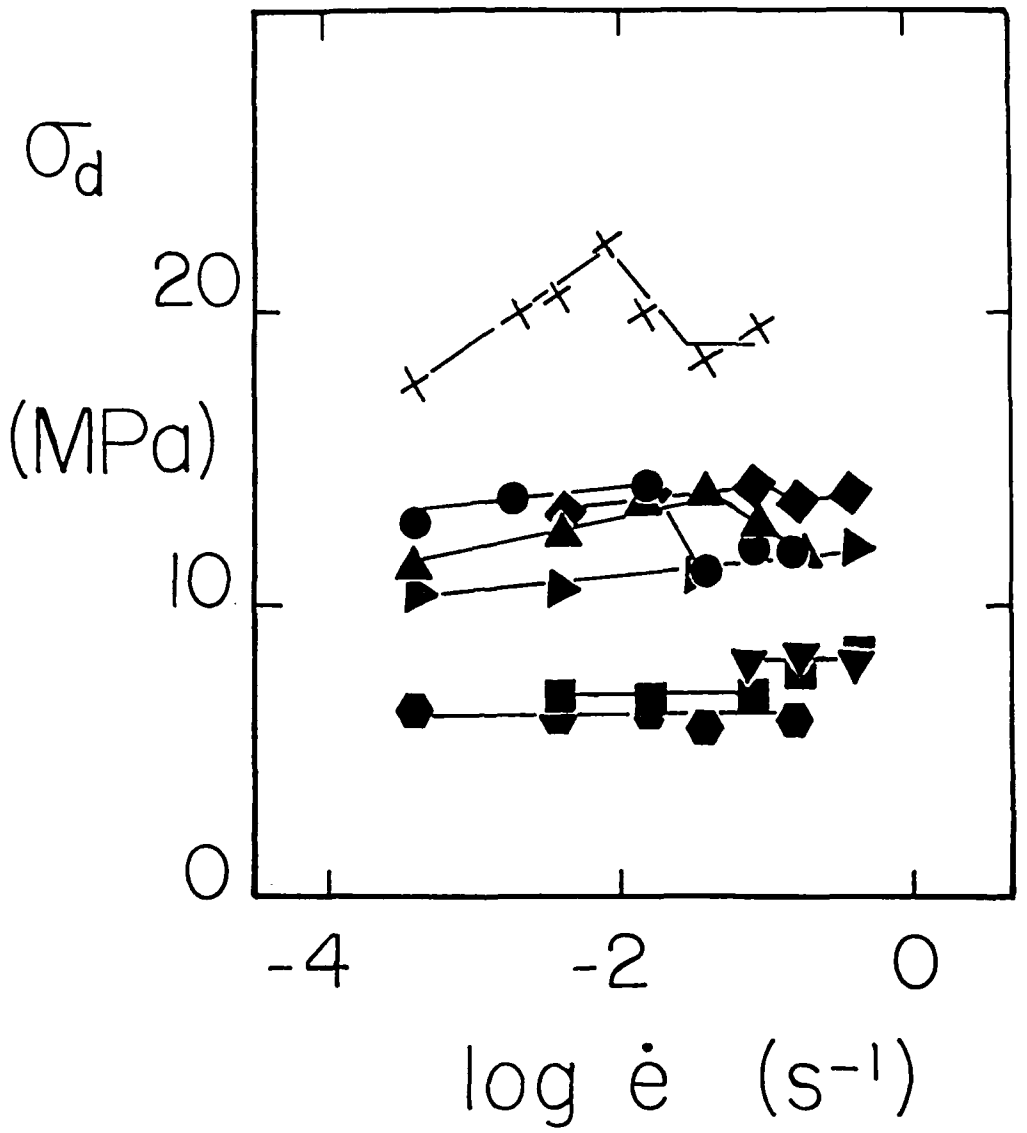

Figure 10

(DYN)

DISTRIBUTION LIST

Dr. R.S. Miller
Office of Naval Research
Code 432P
Arlington, VA 22217
(10 copies)

Dr. J. Pastine
Naval Sea Systems Command
Code 06R
Washington, DC 20362

Dr. Kenneth D. Hartman
Hercules Aerospace Division
Hercules Incorporated
Alleghany Ballistic Lab
P.O. Box 210
Cumberland, MD 20502

Mr. Otto K. Heiney
AFATL-DLJG
Elgin AFB, FL 32542

Dr. Merrill K. King
Atlantic Research Corp.
5390 Cherokee Avenue
Alexandria, VA 22312

Dr. R.L. Lou
Aerojet Strategic Propulsion Co.
Bldg. 05025 - Dept 5400 - MS 167
P.O. Box 15699C
Sacramenta, CA 95813

Dr. R. Olsen
Aerojet Strategic Propulsion Co.
Bldg. 05025 - Dept 5400 - MS 167
P.O. Box 15699C
Sacramento, CA 95813

Dr. Randy Peters
Aerojet Strategic Propulsion Co.
Bldg. 05025 - Dept 5400 - MS 167
P.O. Box 15699C
Sacramento, CA 95813

Dr. D. Mann
U.S. Army Research Office
Engineering Division
Box 12211
Research Triangle Park, NC 27709-2211

Dr. L.V. Schmidt
Office of Naval Technology
Code 07CT
Arlington, VA 22217

JHU Applied Physics Laboratory
ATTN: CPIA (Mr. T.W. Christian)
Johns Hopkins Rd.
Laurel, MD 20707

Dr. R. McGuire
Lawrence Livermore Laboratory
University of California
Code L-324
Livermore, CA 94550

P.A. Miller
736 Leavenworth Street, #6
San Francisco, CA 94109

Dr. W. Moniz
Naval Research Lab.
Code 6120
Washington, DC 20375

Dr. K.F. Mueller
Naval Surface Weapons Center
Code R11
White Oak
Silver Spring, MD 20910

Prof. M. Nicol
Dept. of Chemistry & Biochemistry
University of California
Los Angeles, CA 90024

Mr. L. Roslund
Naval Surface Weapons Center
Code R10C
White Oak, Silver Spring, MD 20910

Dr. David C. Sayles
Ballistic Missile Defense
Advanced Technology Center
P.O. Box 1500
Huntsville, AL 35807

(DYN)

DISTRIBUTION LIST

Mr. R. Geisler
ATTN: DY/MS-24
AFRPL
Edwards AFB, CA 93523

Naval Air Systems Command
ATTN: Mr. Bertram P. Sobers
NAVAIR-320G
Jefferson Plaza 1, RM 472
Washington, DC 20361

R.B. Steele
Aerojet Strategic Propulsion Co.
P.O. Box 15699C
Sacramento, CA 95813

Mr. M. Stosz
Naval Surface Weapons Center
Code R10B
White Oak
Silver Spring, MD 20910

Mr. E.S. Sutton
Thiokol Corporation
Elkton Division
P.O. Box 241
Elkton, MD 21921

Dr. Grant Thompson
Morton Thiokol, Inc.
Wasatch Division
MS 240 P.O. Box 524
Brigham City, UT 84302

Dr. R.S. Valentini
United Technologies Chemical Systems
P.O. Box 50015
San Jose, CA 95150-0015

Dr. R.F. Walker
Chief, Energetic Materials Division
DRSMC-LCE (D), B-3022
USA ARDC
Dover, NJ 07801

Dr. Janet Wall
Code 012
Director, Research Administration
Naval Postgraduate School
Monterey, CA 93943

Director
US Army Ballistic Research Lab.
ATTN: DRXBR-IBD
Aberdeen Proving Ground, MD 21005

Commander
US Army Missile Command
ATTN: DRSMI-RKL
Walter W. Wharton
Redstone Arsenal, AL 35898

Dr. Ingo W. May
Army Ballistic Research Lab.
ARRADCOM
Code DRXBR - IBD
Aberdeen Proving Ground, MD 21005

Dr. E. Zimet
Office of Naval Technology
Code 071
Arlington, VA 22217

Dr. Ronald L. Derr
Naval Weapons Center
Code 389
China Lake, CA 93555

T. Boggs
Naval Weapons Center
Code 389
China Lake, CA 93555

Lee C. Estabrook, P.E.
Morton Thiokol, Inc.
P.O. Box 30058
Shreveport, Louisiana 71130

Dr. J.R. West
Morton Thiokol, Inc.
P.O. Box 30058
Shreveport, Louisiana 71130

Dr. D.D. Dillehay
Morton Thiokol, Inc.
Longhorn Division
Marshall, TX 75670

G.T. Bowman
Atlantic Research Corp.
7511 Wellington Road
Gainesville, VA 22065

(DYN)

DISTRIBUTION LIST

R.E. Shenton
Atlantic Research Corp.
7511 Wellington Road
Gainesville, VA 22065

Mike Barnes
Atlantic Research Corp.
7511 Wellington Road
Gainesville, VA 22065

Dr. Lionel Dickinson
Naval Explosive Ordinance
Disposal Tech. Center
Code D
Indian Head, MD 20340

Prof. J.T. Dickinson
Washington State University
Dept. of Physics 4
Pullman, WA 99164-2814

M.H. Miles
Dept. of Physics
Washington State University
Pullman, WA 99164-2814

Dr. T.F. Davidson
Vice President, Technical
Morton Thiokol, Inc.
Aerospace Group
3340 Airport Rd.
Ogden, UT 84405

Mr. J. Consaga
Naval Surface Weapons Center
Code R-16
Indian Head, MD 20640

Naval Sea Systems Command
ATTN: Mr. Charles M. Christensen
NAVSEA-62R2
Crystal Plaza, Bldg. 6, Rm 806
Washington, DC 20362

Mr. R. Beauregard
Naval Sea Systems Command
SEA 64E
Washington, DC 20362

Brian Wheatley
Atlantic Research Corp.
7511 Wellington Road
Gainesville, VA 22065

Mr. G. Edwards
Naval Sea Systems Command
Code 62R32
Washington, DC 20362

C. Dickinson
Naval Surface Weapons Center
White Oak, Code R-13
Silver Spring, MD 20910

Prof. John Deutch
MIT
Department of Chemistry
Cambridge, MA 02139

Dr. E.H. deButts
Hercules Aerospace Co.
P.O. Box 27408
Salt Lake City, UT 84127

David A. Flanigan
Director, Advanced Technology
Morton Thiokol, Inc.
Aerospace Group
3340 Airport Rd.
Ogden, UT 84405

Dr. L.H. Caveny
Air Force Office of Scientific
Research
Directorate of Aerospace Sciences
Bolling Air Force Base
Washington, DC 20332

W.G. Roger
Code 5253
Naval Ordance Station
Indian Head, MD 20640

Dr Donald L. Ball
Air Force Office of Scientific
Research
Directorate of Chemical &
Atmospheric Sciences
Bolling Air Force Base
Washington, DC 20332

(DYN)

DISTRIBUTION LIST

Dr. Anthony J. Matuszko
Air Force Office of Scientific Research
Directorate of Chemical & Atmospheric Sciences
Bolling Air Force Base
Washington, DC 20332

Dr. Michael Chaykovsky
Naval Surface Weapons Center
Code R11
White Oak
Silver Spring, MD 20910

J.J. Rocchio
USA Ballistic Research Lab.
Aberdeen Proving Ground, MD 21005-5066

B. Swanson
INC-4 MS C-346
Los Alamos National Laboratory
Los Alamos, New Mexico 87545

Dr. James T. Bryant
Naval Weapons Center
Code 3205B
China Lake, CA 93555

Dr. L. Rothstein
Assistant Director
Naval Explosives Dev. Engineering Dept.
Naval Weapons Station
Yorktown, VA 23691

Dr. M.J. Kamlet
Naval Surface Weapons Center
Code R11
White Oak, Silver Spring, MD 20910

Dr. Henry Webster, III
Manager, Chemical Sciences Branch
ATTN: Code 5063
Crane, IN 47522

Dr. A.L. Slafkosky
Scientific Advisor
Commandant of the Marine Corps
Code RD-1
Washington, DC 20380

Dr. H.G. Adolph
Naval Surface Weapons Center
Code R11
White Oak
Silver Spring, MD 20910

U.S. Army Research Office
Chemical & Biological Sciences Division
P.O. Box 12211
Research Triangle Park, NC 27709

Dr. John S. Wilkes, Jr.
FJSRL/NC
USAF Academy, CO 80840

Dr. H. Rosenwasser
AIR-320R
Naval Air Systems Command
Washington, DC 20361

Dr. Joyce J. Kaufman
The Johns Hopkins University
Department of Chemistry
Baltimore, MD 21218

Dr. A. Nielsen
Naval Weapons Center
Code 385
China Lake, CA 93555

(DYN)

DISTRIBUTION LIST

K.D. Pae
High Pressure Materials Research Lab.
Rutgers University
P.O. Box 909
Piscataway, NJ 08854

Dr. John K. Dienes
T-3, B216
Los Alamos National Lab.
P.O. Box 1663
Los Alamos, NM 87544

A.N. Gent
Institute Polymer Science
University of Akron
Akron, OH 44325

Dr. D.A. Shockey
SRI International
333 Ravenswood Ave.
Menlo Park, CA 94025

Dr. R.B. Kruse
Morton Thiokol, Inc.
Huntsville Division
Huntsville, AL 35807-7501

G. Butcher
Hercules, Inc.
P.O. Box 98
Magna, UT 84044

W. Waesche
Atlantic Research Corp.
7511 Wellington Road
Gainesville, VA 22065

Dr. R. Bernecker
Naval Surface Weapons Center
Code R13
White Oak
Silver Spring, MD 20910

Prof. Edward Price
Georgia Institute of Tech.
School of Aerospace Engineering
Atlanta, GA 30332

J.A. Birkett
Naval Ordnance Station
Code 5253K
Indian Head, MD 20640

Prof. R.W. Armstrong
University of Maryland
Dept. of Mechanical Engineering
College Park, MD 20742

Herb Richter
Code 385
Naval Weapons Center
China Lake, CA 93555

J.T. Rosenberg
SRI International
333 Ravenswood Ave.
Menlo Park, CA 94025

G.A. Zimmerman
Aeroject Tactical Systems
P.O. Box 13400
Sacramento, CA 95813

Prof. Kenneth Kuo
Pennsylvania State University
Dept. of Mechanical Engineering
University Park, PA 16802

T.L. Boggs
Naval Weapons Center
Code 3891
China Lake, CA 93555

(DYN)

DISTRIBUTION LIST

Dr. C.S. Coffey
Naval Surface Weapons Center
Code R13
White Oak
Silver Spring, MD 20910

D. Curran
SRI International
333 Ravenswood Avenue
Menlo Park, CA 94025

E.L. Throckmorton
Code SP-2731
Strategic Systems Program Office
Crystal Mall #3, RM 1048
Washington, DC 23076

R.G. Rosemeier
Brimrose Corporation
7720 Belair Road
Baltimore, MD 20742

C. Gotzmer
Naval Surface Weapons Center
Code R-11
White Oak
Silver Spring, MD 20910

G.A. Lo
3251 Hanover Street
B204 Lockheed Palo Alto Research Lab
Palto Alto, CA 94304

R.A. Schapery
Civil Engineering Department
Texas A&M University
College Station, TX 77843

Dr. Y. Gupta
Washington State University
Department of Physics
Pullman, WA 99163

J.M. Culver
Strategic Systems Projects Office
SSPO/SP-2731
Crystal Mall #3, RM 1048
Washington, DC 20376

Prof. G.D. Duvall
Washington State University
Department of Physics
Pullman, WA 99163

Dr. E. Martin
Naval Weapons Center
Code 3858
China Lake, CA 93555

Dr. M. Farber
135 W. Maple Avenue
Monnovia, CA 91016

W.L. Elban
Naval Surface Weapons Center
White Oak, Bldg. 343
Silver Spring, MD 20910

Defense Technical Information Center
Bldg. 5, Cameron Station
Alexandria, VA 22314
(12 copies)

Dr. Robert Polvani
National Bureau of Standards
Metallurgy Division
Washington, D.C. 20234

Director
Naval Research Laboratory
Attn: Code 2627
Washington, DC 20375
(6 copies)

Administrative Contracting
Officer (see contract for
address)
(1 copy)